

Posttranslationally Processed Forms of the Human Chemokine HCC-1

Rudolf Richter,* Peter Schulz-Knappe, Harald John, and Wolf-Georg Forssmann

Lower Saxony Institute for Peptide Research, Feodor-Lynen Strasse 31, D-30625 Hannover, Germany

Received October 26, 1999; Revised Manuscript Received March 28, 2000

ABSTRACT: HCC-1 is the only CC-chemokine known so far which circulates in nanomolar concentrations in human plasma. Its physiological function is not well defined. Posttranslational processing of HCC-1 was shown to modulate its biological properties. In this study several different processed forms of HCC-1 were isolated. Western blot analysis of human plasma extracts revealed a HCC-1 immunoreactive double band at 8–10 kDa indicating the presence of two distinct HCC-1 peptides. These peptides were isolated from a peptide library of human blood filtrate and represent predominantly HCC-1 (1–74) and glycosylated HCC-1 (1–74). Glycosylated HCC-1 exhibits a molecular mass of 9621 Da due to O-glycosylation at position 7 (Ser-7) with two *N*-acetylneuraminic acids and the disaccharide *N*-acetylgalactosamine galactose. Furthermore N-terminally truncated HCC-1 (3–74) and HCC-1 (4–74) were identified in the peptide library. In hemofiltrate approximately 3% of total HCC-1 represents HCC-1 (3–74) and approximately 1% represents HCC-1 (4–74) whereas the major products are nonglycosylated HCC-1 (1–74) and glycosylated HCC-1 (1–74). Our data imply that HCC-1 (1–74), HCC-1 (3–74), HCC-1 (4–74) and glycosylated HCC-1 (1–74) circulate in human blood. The N-terminal processing and modification of HCC-1 might be of importance in displaying its full biological activity.

HCC-1 is a CC chemokine isolated from human hemofiltrate (HF)¹ (1). Mature HCC-1 exhibits a high sequence identity to macrophage inflammatory protein (MIP)-1 α and MIP-1 β . Investigation of biological activities of HCC-1 revealed significant differences to other CC-chemokines (2). At high nanomolar concentrations HCC-1 induces an increase in intracellular Ca²⁺ and a slight but significant release of *N*-acetyl- β -D-glucosaminidase activity from monocytes (1). HCC-1 stimulates weakly chemotactic responses of monocytes (3). It enhances the proliferation of CD34+ cells but is markedly less potent than MIP-1 α (1). It is suggested, that HCC-1 specifically activates CC chemokine receptor-1

(CCR-1) (3). HCC-1 competes with MIP-1 α in binding to CCR-1-transfected cells, but with a perceptibly reduced affinity. Uncommon for other CC-chemokines, HCC-1 is constitutively expressed in several normal tissues such as spleen, liver, skeletal and heart muscle, gut and bone marrow and is present at extremely high concentrations in plasma (1). No expression is observed in leukocytes or monocytic cell lines. The high plasma levels suggest systemic effects of HCC-1 rather than local chemotactic effects. Tsou and co-workers demonstrated that the N-terminally truncated HCC-1 induces a stronger chemotactic activity than the mature HCC-1 (1–74) (3). The present study was performed in order to identify different endogenous molecular modifications of HCC-1, supporting the hypothesis that posttranslational processing of HCC-1 is of importance for its biological activity.

MATERIALS AND METHODS

Generation of Polyclonal Anti-HCC-1 Antibodies. Immunization of the rabbit (K110) was performed using a multiple antigenic peptide consisting of a branched heptalysine core with eight copies of the carboxyl-terminal domain of HCC-1 (Asp⁶²-Asn⁷⁴) as described by Schulz-Knappe et al. (1). The antibody was used for Western blot analysis. For immunization of the chicken (C2), the animal was injected into the pectoral muscles with 100 μ g native HCC-1 (1–74) dissolved in 0.5 mL of 0.1 M sodium acetate, pH 6.3, emulsified in 0.5 mL complete Freund's adjuvant (Calbiochem, Nottingham, UK). The chicken was boosted three times at intervals of 4 weeks with 100 μ g HCC-1 in 0.5 mL of 0.1 M sodium acetate, pH 6.3, emulsified in 0.5 mL incomplete Freund's adjuvant (Difco Laboratories, Augsburg, Germany). The antibodies were isolated from the egg yolk according

* To whom correspondence should be addressed. Phone: +49-(0)-511-5466-523. Fax: +49-(0)-511-5466-132. E-mail: rudorichter@gmx.de.

¹ Abbreviations: API, atmospheric pressure ionization; BNP, brain natriuretic peptide; CD, cluster of differentiation; CCR-1, CC chemokine receptor-1; CNP, C-type natriuretic peptide; Da, Dalton; DTT, dithiothreitol; ELC, EB11-ligand chemokine; HCC, hemofiltrate CC-chemokine; CDD/ANP, cardiodilatin/atrial natriuretic peptide; ESMS, electrospray ionization mass spectrometry; Gal, galactose; GalNAc, *N*-acetylgalactosamine; GM-CSF, granulocyte-macrophage colony-stimulating factor; HPAE-PAD, high performance anion exchange/pulsed amperometric detection chromatography; IL-8, interleukin-8; IP10, 10-kDa inflammatory protein; IR, immunoreactive; HEK, human embryonic kidney cell; HF, hemofiltrate; HUH-7, human hepatoma cell line; LARC, liver and activation-regulated chemokine; LC-MS, liquid chromatography–mass spectrometry; MALDI-MS, matrix-assisted laser desorption ionization–mass spectrometry; MCP, monocyte chemoattractant protein; MIP-1 α , macrophage inflammatory protein-1 α ; MIPF, myeloid progenitor inhibitory factor; NANA, *N*-acetylneuraminic acid; PEG, poly(ethylene glycol); PACAP, pituitary adenylate cyclase-activating polypeptide; PBMC, peripheral blood mononuclear cells; PTH, phenyl-thiohydantoin; PVDF, poly(vinylidene difluoride); RANTES, regulated on activation, normal T cell expressed and secreted chemokine; RT, room temperature; SDF-1 α , stromal cell-derived factor-1 α ; TARC, thymus and activation-regulated chemokine; VIP, vasoactive intestinal peptide.

to the method of Polson et al. (4) and used for establishing a RIA.

Radioimmunoassay. Native HCC-1 was radio-iodinated using the chloramine-T method. 2 μ L of a 125 I-solution (200 μ Ci 125 I, Amersham, Buckinghamshire, UK) were added to 1 μ g HCC-1 (1–74) in 75 μ L of 0.25 M sodium phosphate buffer, pH 7.4. The reaction was initiated by the addition of 10 μ L chloramine-T solution (1 mg/mL in phosphate buffer). The mixture was allowed to react for 60 s and the reaction was stopped by the addition of 10 μ L sodium thiosulfate solution (2.5 mg/mL phosphate buffer). SepPak C18 cartridges (Waters, Milford, MA) were used to separate labeled peptide from free 125 I. Bound peptides were eluted using 0.01 M HCl in 80% acetonitrile. Specific activity was calculated at 100 μ Ci/ μ g. 140 mM sodium phosphate buffer, pH 6.0, containing 171 mM NaCl, 43 mM citric acid, 0.5% w/v bovine serum albumin (Fraction V; Sigma, Deisenhofen, Germany), 1 mM dithiothreitol, 5 mM EDTA, 0.05% v/v Tween 20, and 0.05% w/v NaN_3 was used as RIA buffer. All reagents and samples were dissolved in RIA buffer. The incubation mixture consisted of 100 μ L sample or standard, 100 μ L of 1:1600 dilution of purified chicken antibody C2, and 100 μ L of a 125 I–HCC-1 solution (20,000 cpm/100 μ L). The incubation was performed for 18 to 24 h. The bound and free antigens were separated by incubation with 100 μ L donkey anti-chicken-IgG γ -globulin (Immundiagnostik, Bensheim, Germany), 100 μ L 15% w/v poly(ethylene glycol) (PEG-6000) for 2 h, prior to centrifugation at 2500 g for 30 min. Subsequently the pellets of the samples and standards were washed with 500 μ L PBS, containing 6% w/v PEG-6000. After centrifugation the radioactivity of the precipitate was counted in a γ -spectrometer (Wallac, Freiburg, Germany). All steps were performed at RT. The calibration curve was calculated using B/B₀ vs fmol of HCC-1.

Western Blot Analysis. For immunoblots, aliquots of peptide library fractions were lyophilized and resuspended in sample buffer containing 1% w/v sodium dodecyl sulfate (Merck, Darmstadt, Germany), 7.5 mM Tris-HCl, pH 8.4, 1 mM EDTA, 32.4 mM dithiothreitol (Roth, Germany), 12.5% w/v glycerol (Merck) and 0.025% w/v bromophenol blue (Merck) and incubated for 7 min at 95 °C (reducing conditions). The samples were separated by tricine-SDS–PAGE in 17.5% gels (5). HCC-1 (1–74) and glycosylated HCC-1 (1–74), isolated from hemofiltrate, were used as external standards. After electrophoresis, proteins were electroblotted onto hydrophobic poly(vinylidene difluoride) (PVDF)-based membranes (Pall, Dreieich, Germany). To minimize nonspecific binding of the antibodies, blot strips were incubated with 5% w/v FCS in Tris-buffered saline (10 mM Tris, 150 mM NaCl, pH 8.0) and 0.05% v/v Triton X 100 (TBST). After washing in TBST the membranes were incubated overnight at 4 °C with rabbit K110 antiserum diluted in TBST (1:2000). Immunoreactive proteins were visualized after incubation with alkaline phosphatase-blue tetrazolium and 5-bromo-4-chloro-3-indolyl phosphate as chromogens (Sigma). Proteins remaining in the gels were fixed in 30% methanol and 10% acetic acid for 45 min before staining with Coomassie brilliant blue in 10% acetic acid for 1–2 h.

Analysis of IR–HCC-1 in Human Plasma. IR–HCC-1 in human plasma was identified by chromatography of 1 mL plasma on a preparative reverse phase (RP) – HPLC, 250

mm \times 10 mm inside diameter, Source RPC 15 (Pharmacia, Uppsala, Sweden) with a gradient from 100% solvent A (0.1% v/v TFA) to 100% solvent B (100% acetonitrile, 0.1% v/v TFA) in 50 min using a flow rate of 2 mL/min. Obtained fractions were analyzed by the HCC-1 RIA. For further analysis of IR–HCC-1 200 mL fresh frozen plasma were ultrafiltrated using a MiniPlate Biocentrator (Amicon, Beverly, MA) with a specified molecular mass cutoff of 30 kDa. The filtrate was loaded onto a RP column, Source RPC, 250 mm \times 20 mm inside diameter, 15 μ m (Pharmacia), and batch eluted using 0.1% v/v TFA in 80% acetonitrile. The eluate was lyophilized and rechromatographed on an analytical Superdex G 75 gel-chromatography column (800 mm \times 16 mm inside diameter; Pharmacia), using a buffer of 50 mM NaH_2PO_4 , pH 8.9 with a flow rate of 1 mL/min. The immunoreactive fractions were pooled and rechromatographed on a RP column, Source RPC, 250 mm \times 20 mm inside diameter, 15 μ m (Pharmacia) with a linear gradient from 100% A (0.1% v/v TFA) to 60% solvent B (0.1% v/v TFA in 80% acetonitrile) and a flow rate of 2 mL/min. Fractions of 2 mL were collected. All fractions which revealed IR–HCC-1 were analyzed by MALDI-MS and Western blot.

Generation of a Hemofiltrate Peptide Library. Human hemofiltrate for large scale recovery of plasma peptides (6) was obtained from patients with chronic renal failure in quantities of 1600 to 2000 L per week. Ultrafilters used for hemofiltration had a specified molecular mass cutoff of 20 kDa. The sterile filtrate was immediately cooled to 4 °C and acidified to pH 3 to prevent bacterial growth and proteolysis. For peptide extraction batches of 1000 L HF were conditioned to pH 2.7 and applied onto the strong cation exchanger, Fractogel TSK SP 650(M), 100 mm \times 250 mm (Merck, Darmstadt, Germany) using an Autopilot chromatography system (PerSeptive Biosystems, Wiesbaden, Germany) (7). Batch elution was performed with 10 L 0.5 M ammonium acetate. The eluate was stored at –20 °C until further use. The peptide library was produced as described by Schulz-Knappe et al. (7). Briefly, for the first separation step the extracts of 5000 L HF were pooled and loaded on a 10 L cation exchange column (Fractogel SP 650(M); Merck). Bound peptides were eluted using seven buffers with increasing pH resulting in seven pH-pools. The seven buffers were composed as follows: I: 0.1 M citric acid monohydrate, pH 3.6; II: 0.1 M acetic acid + 0.1 M sodium acetate, pH 4.5; III: 0.1 M malic acid, pH 5.0; IV: 0.1 M succinic acid, pH 5.6; V: 0.1 M sodium dihydrogen phosphate, pH 6.6; 0.1 M disodiumhydrogen phosphate, pH 7.4; VII: 0.1 M ammonium carbonate, pH 9.0. The seven pools (pH pools) were collected and each of them was loaded onto a RP column, 125 mm \times 100 mm inside diameter, Source RPC, 15 μ m (Pharmacia) and eluted in a 8 L gradient from 100% A (0.01 M HCl in water) to 60%B (0.01 M HCl in 80% acetonitrile). Fractions of 200 mL were collected.

Peptide Purification from Human Hemofiltrate. Fractions containing IR–HCC-1 were detected by HCC-1 RIA and Western blot analysis. Glycosylated HCC-1 was further purified to homogeneity by 4 consecutive chromatographic steps A to D. (A) Preparative RP–C18 chromatography of IR–HCC-1 fractions of pH-Pool VI. Column: Vydac PrepPak RP–C18, 300 mm \times 47 mm inside diameter, 15–20 μ m, 300 Å (Vydac, Hesperia, USA). Three identical

separations were performed at a flow rate of 40 mL/min using a linear binary gradient of 70% solvent A (0.1% v/v TFA in water) to 100% solvent B (0.1% v/v TFA in methanol) in 50 min. Fractions of 50 mL were collected. (B) Preparative RP-C18 chromatography of the active fractions from step A. Column: Bakerbond PrepPak RP-C18, 300 mm \times 47 mm inside diameter, 15–30 μ m, 300 Å (Waters). Separation was performed at a flow rate of 40 mL/min using a linear binary gradient of 80% solvent A (10 mM HCl in water) to 50% solvent B (10 mM HCl in 80% acetonitrile) in 30 min. Fractions of 50 mL were collected. (C) Analytical RP-C18 chromatography of the active fractions from step B. Column: YMC RP-C18 AQ, 250 mm \times 10 mm inside diameter, 5 μ m, 120 Å (YMC, Schermbeck, Germany). Separation was performed at a flow rate of 2 mL/min using a linear binary gradient from 80% solvent A (10 mM HCl in water) to 50% solvent B (10 mM HCl in 80% acetonitrile) within 50 min. (D) Cation exchange chromatography of the active fractions from step C. Column: Ultropac TSK 535 CMC 150 mm \times 7 mm inside diameter (Pharmacia). Separation was performed at a flow rate of 1.5 mL/min using a linear binary gradient from 100% buffer A (50 mM sodium acetate, pH 4.6) to 100% buffer B (50 mM sodium acetate, pH 4.6, 1 M NaCl) within 75 min. Fractions were desalted by solid-phase extraction using SepPak-Cartridges (Waters) and 0.1% v/v TFA in 80% acetonitrile as eluent. Isolation of HCC-1 (3–74) and HCC-1 (4–74) was performed by comparable isolation procedures.

Protease Digestion. The isolated native HCC-1 (1–74) and glycosylated HCC-1 (1–74) underwent proteolytic fragmentation by overnight-incubation with trypsin (EC 3.4.21.4) in a protein: peptidase ratio of 50:1 w/w. The reaction was stopped by boiling and fragments were separated by microbore HPLC (Smart System, Pharmacia) using a RP-C18 column (100 mm \times 1 mm inside diameter, ODS-AQ, 3 μ m, 120 Å, YMC, Schermbeck, Germany). Eluting peptides were collected using the in-built micro-fraction collector.

Carbohydrate Analysis. Analysis of the carbohydrate composition was performed using different deglycosylating enzymes: 25 μ g of the glycosylated HCC-1 (1–74) were incubated with neuraminidase from *Vibrio cholerae* (EC 3.2.1.18; 0.1 U; Boehringer Mannheim, Germany), neuraminidase plus O-glycosidase from *Diplococcus pneumoniae* (EC 3.2.1.97; 12 mU, Boehringer Mannheim, Germany) or with glycopeptidase F alone (200 mU) at 37 °C for 24 h. Following incubation samples were analyzed by MALDI-MS and amino-sugar analysis using high performance anion exchange/pulsed amperometric detection (HPAE-PAD)-chromatography (Dionex, Salt Lake City, USA) using external standards for identification.

Mass Spectrometry and LC-MS Coupling. ESMS was carried out on an API III Triple stage quadrupole mass spectrometer equipped with the articulated ion spray (Perkin-Elmer SCIEX, Langen, Germany). Flow injection was carried out at 5 μ L/min. The masses were determined in the range from 400 to 2300 Da in the positive ion mode as described by the manufacturer. The peptide masses were calculated using the MacSpec 3.3 software (Perkin-Elmer, Langen, Germany).

LC-ESMS coupling was performed using a Microbore RP-HPLC and an ABI Model 140 B Dual Syringe Solvent

Delivery System, equipped with an ABI Model 785 Programmable Absorbance Detector (Applied Biosystems, Weiterstadt, Germany) with capillary Z-cell (LC-Packings, Amsterdam, The Netherlands). A Rheodyne Model 8125 injection valve with a 5 μ L loop was used. Separations were carried out with a C18 column, 100 mm \times 1 mm inside diameter, ODS-AQ, 3 μ m, 120 Å, (YMC, Schermbeck, Germany). The column outlet was connected to the electrospray interface of the API III mass spectrometer using a fused silica capillary with an inside diameter of 50 μ m. Separations were performed at a flow rate of 20 μ L/min using a linear gradient of 10% solvent A (0.06% v/v TFA in water) to 60% solvent B (0.05% v/v TFA in 80% acetonitrile) in 90 min. On-line mass analysis was performed at 5,000 V interface voltage and 70 to 100 V orifice voltage, scans ranged from 300 to 2300 Da with 0.3 Da steps and 0.1 ms measurement dwell time for each step. All analyses were performed under single MS conditions, using the first quadrupole as mass filter.

MALDI-MS was performed using a LaserTec RBT matrix assisted laser desorption ionization-mass spectrometer (PerSeptive/Vestec, Texas, US). Isolated HCC-1 was applied to a stainless steel multiple sample tray as an admixture to sinapinic acid using the dried drop technique (8). Measurements were performed in linear mode. The instrument was equipped with a 1.2 m flight tube and a 337 nm nitrogen laser. Positive ions were accelerated at 30 kV and 64 laser shots were automatically accumulated per sample position. The time-of-flight data were externally calibrated for each sample plate and sample preparation. Data acquisition and analysis were performed using GRAMS 386 version 3.04 software supplied by the manufacturer.

Sequence Analysis. Sequence analyses of the isolated peptides were performed by stepwise Edman degradation using a gas-phase automated sequencer (Model 473 A, Applied Biosystems; Weiterstadt, Germany). The resulting PTH-amino acids were identified by integrated HPLC.

RESULTS

HCC-1 RIA and HCC-1 Western Blot Analysis. In the RIA the detection limit of HCC-1 was 0.98 fmol/tube. The binding of 125 I-HCC-1 in the absence of unlabeled HCC-1 was $16.3 \pm 1.7\%$. The intercept 50 was found to be 62.5 fmol/tube. The intra- and interassay coefficients of variation were 15% and 20%, respectively. The dilution curves generated from human plasma paralleled that of standard HCC-1. The used antiserum C2 does not cross-react with the CC chemokines ELC, TARC, LARC, Eotaxin, I-309, MCP-1, MIP-1, MIP-1 β , RANTES or MCP-3 or CXC-chemokines IL-8, IP10, SDF-1 α , nor with other hormones (GM-CSF, substance P, CDD/ANP-99–126, BNP, CNP, neurotensin, PACAP-1–27, PACAP-1–38, angiotensin I, angiotensin II, neurokinin A, VIP, bombesin, bradykinin, neurokinin B). The HCC-1 splice variant HCC-3 as well as the newly identified HCC-1 (3–74), HCC-1 (4–74) and glycosylated HCC-1 (1–74) show a 100% cross-reaction in the RIA. HCC-2 cross react of 0.6% and MIP-1 α shows a cross-reaction of 0.1%.

In Western blot analysis the antibody K110 showed no cross-reactivity with the CC chemokines ELC, TARC, LARC, Eotaxin, I-309, MCP-1, MIP-1, MIP-1 β , RANTES, HCC-2 or MCP-3 or CXC-chemokines IL-8, IP10, SDF-

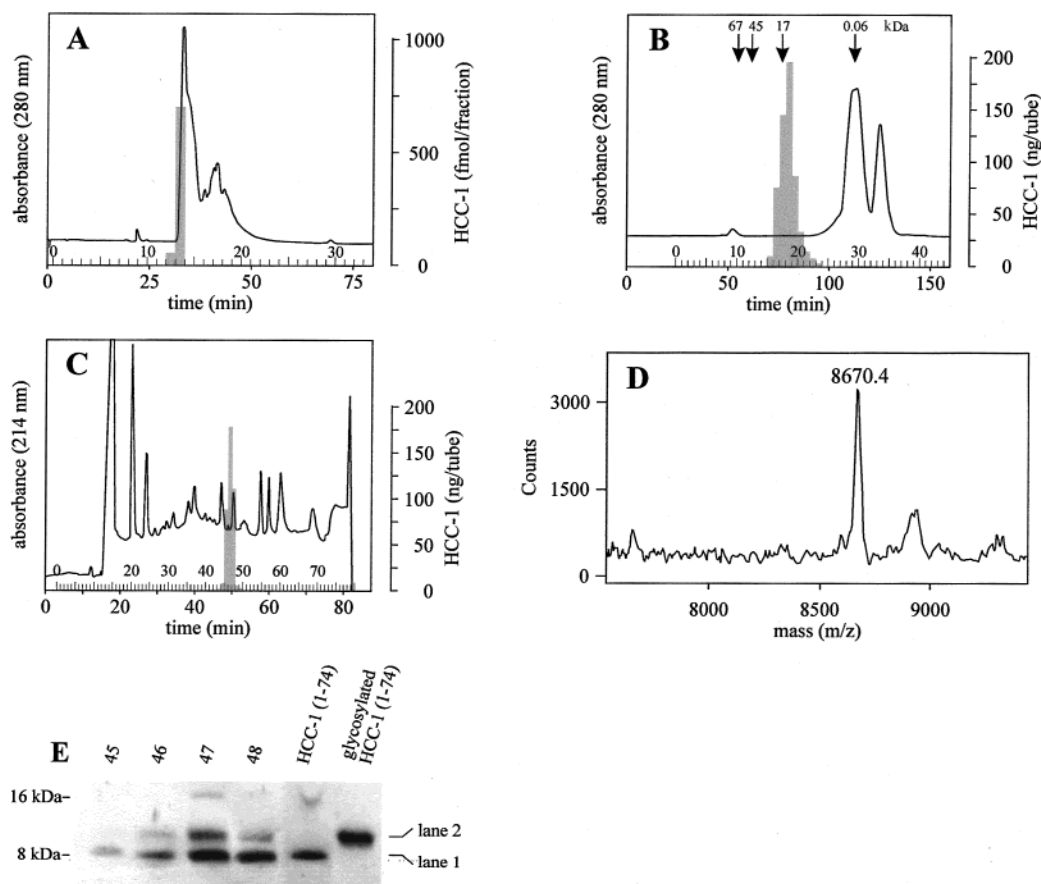


FIGURE 1: Analysis of IR-HCC-1 in human plasma. The shaded area represents IR-HCC-1 in the chromatographic fractions, detected by RIA. Experimental conditions are detailed in Materials and Methods. (A) RP-HPLC of 1 mL of plasma. A representative purification is shown. (B + C) Purification of IR-HCC-1 from human plasma. (B) Size exclusion chromatography of plasma ultrafiltrate. A total of 200 mL of fresh frozen plasma was ultrafiltered. The filtrate was desalted and lyophilized and loaded onto a Superdex G 75 gel-chromatography column and chromatographed using a buffer of 50 mM NaH_2PO_4 , pH 8.9. IR-HCC-1 was found in fractions 16–24. (C) RP-chromatography of immunoreactive fractions shown in panel B. IR-HCC-1 was predominantly found in fractions 46–48. (D) MALDI-MS of immunoreactive fraction 47 shown in panel C exhibits a molecular mass of 8670.4 ± 3.5 Da, which is in accordance to the theoretical average mass of 8673.7 Da for HCC-1 (1–74). (E) Western blot analysis of fractions 45–48 of the RP-chromatography shown in panel C. Purified native HCC-1 (1–74) and glycosylated HCC-1 (1–74) are used as standards.

1 α . Glycosylated HCC-1, the HCC-1 splice variant HCC-3 as well as the N-terminally truncated forms of HCC-1 revealed high cross-reactivity to the antibody K110.

Analysis of Immunoreactive HCC-1 in Human Plasma. Analysis of human plasma from healthy donors as well as patients with chronic renal failure using RP chromatography and HCC-1 RIA revealed a single peak of IR-HCC-1 (Figure 1A). Further analysis was performed by purification of IR-HCC-1 from fresh frozen plasma using ultrafiltration, size exclusion chromatography, and RP chromatography. Main IR-HCC-1 was identified in fractions 46 to 48 of the RP chromatography (Figure 1C). MALDI-MS analysis of these fractions revealed a molecular mass of 8670.4 ± 3.5 Da which is in accordance with the theoretical average Mw of 8673.7 Da of HCC-1 (1–74) (Figure 1D). Western blot analysis showed a double band (lane 1 and lane 2 in Figure 1E) with an apparent molecular weight of 8–10 kDa. Comparing the relative mobility of both lanes with that of purified HCC-1 (1–74) as well as purified glycosylated HCC-1 (1–74) suggests that lane 2 most likely represents glycosylated HCC-1 whereas lane 1 represents the nonglycosylated form of HCC-1 (Figure 1E).

Purification and Analysis of Immunoreactive HCC-1 in Human Hemofiltrate. Extraction of peptides from 5000 L

of human hemofiltrate by cation exchange chromatography resulted in the generation of pH-pool fractions (Figure 2A) which were used in establishing a peptide library of circulating peptides by RP-HPLC. Using the HCC-1 RIA, in the peptide library, IR-HCC-1 was detected predominantly in fractions 11 to 20 of the RP chromatography of pH pool VI (Figure 2B), in fractions 11 to 21 of the RP chromatography of pH pool VII (Figure 2C) and in lower quantities in the RP chromatographies of pH pool IV and V. Using Western blot analysis, IR-HCC-1 was detected in the corresponding RP-fractions of pH pool VI and pH pool VII. Glycosylated HCC-1 was identified in pH pool VI fractions 14 to 18 which showed the double band (Figure 2D) with apparent molecular weights of 8–10 kDa in Western blot analysis.

To elucidate the nature of the double band of the immunoreactive fractions 15 to 18 of pool VI were chromatographed on a preparative RP-HPLC column. Fractions containing IR-HCC-1 (lane 2) were pooled and rechromatographed on the same RP-HPLC column. Fraction 10 positive for IR-HCC-1 (lane 2) was purified on an analytical RP-HPLC column and subsequently chromatographed using an analytical cation exchange column. The fractions were desalted using an analytical RP C_4 column. HCC-1 was identified by N-terminal amino acid sequencing. The mo-

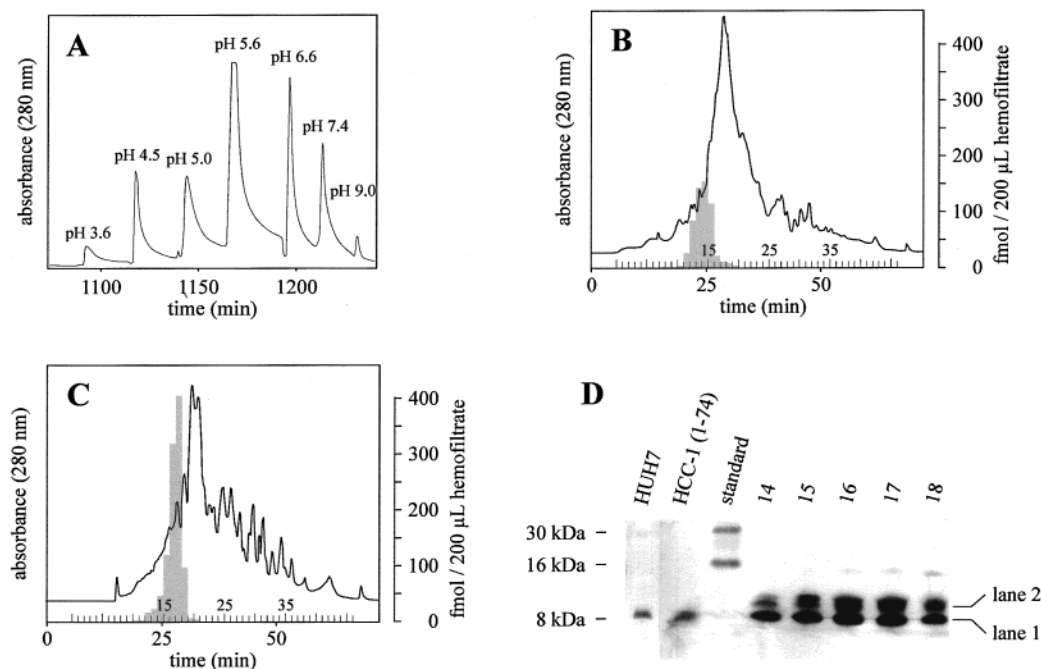


FIGURE 2: Detection of IR-HCC-1 in the hemofiltrate peptide library. Experimental conditions are detailed in Materials and Methods. (A) Stepwise cation exchange chromatography of 5000 L of human hemofiltrate. (B + C) Each pH pool was fractionated by RP-HPLC. Fractions with IR-HCC-1 are marked with shaded columns. IR-HCC-1 was detected by HCC-1 RIA. (B) RP-HPLC of pH pool VI (pH 7.4) and (C) pH pool VII (pH 9.0). IR-HCC-1 was also found in RP-HPLC fractions of pH pool IV and pH pool V (data not shown). (D) Western blot analysis of fractions 14–18 derived from RP chromatography of pH pool VI of human hemofiltrate using the anti-human HCC-1 rabbit antiserum K110. Two major HCC-1 immunoreactive bands were visualized: lane 1 corresponds to HCC-1 (1–74) and lane 2 corresponds to glycosylated HCC-1. Native HCC-1 (1–74) (purity > 95%) was used as reference. IR-HCC-1 in the supernatant of the HUH-7 cell line appears with isolated HCC-1 (1–74). The HUH-7 supernatant was subjected to 0.1 M acetic acid and boiled for 10 min. Extraction of the supernatant was performed using a RP SepPak cartridge.

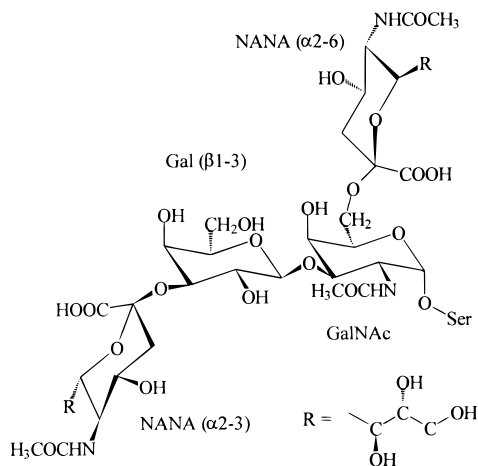


FIGURE 3: Proposed glycosidic side chain of glycosylated HCC-1.

lecular mass of the isolated peptide measured by ESMS was found to be $9,621.7 \pm 1.9$ Da, a difference of 946 Da to that of HCC-1 (1–74). Surprisingly, during sequence analysis no PTH-amino acid was identified in degradation cycle 7, whereas the following residues again matched the HCC-1 sequence. Therefore a side chain modification of the serine in position 7 was assumed to be, at least in part, responsible for this difference in mass. Tryptic digestion of HCC-1 (1–74) and glycosylated HCC-1 (1–74) and Microbore-RP-HPLC chromatograms of these tryptic digests confirmed this result. Comparison of the chromatograms revealed that one major peak was shifted to a shorter retention time. Sequence analysis and mass determination of this peak and of other tryptic fragments confirmed the $\Delta 946$ in the fragment HCC-1

(3–24) TESSSRGPYHPSECCFTYTTYK. Since Ser-7 represents a likely consensus motif for O-glycosylation, the peptide was treated with neuraminidase and O-glycosidase. Samples were measured by MALDI-MS and by HPAE-PAD-chromatography. Neuraminidase treatment resulted in a reduction of the glycosylated HCC-1 (1–74) peptide mass by 582.6 Da corresponding to the cleavage of two neuraminic acid residues (NANA = 291 Da). Subsequent hydrolysis with O-glycosidase resulted in a further reduction of the peptide mass by 364 Da corresponding to a disaccharide consisting of a hexose (galactose, 161 Da) and *N*-acetylhexosamine (*N*-acetylgalactosamine, 203 Da) (Table 1). Glycopeptidase-F-treatment did not result in a mass difference. Sequencing of the peptide after neuraminidase and glycosidase treatment showed the native HCC-1 sequence including the serine residue in position 7 (data not shown).

To evaluate whether HCC-1 is produced solely as glycosylated peptide, IR-HCC-1 was analyzed in cell culture supernatant and cell lysates of the human hepatoma cell line HUH-7 by Western blotting. In the supernatant, only nonglycosylated IR-HCC-1 was detected (Figure 2D) whereas HUH-7 cell lysates did not contain IR-HCC-1 (data not shown).

N-terminally truncated HCC-1 molecules were isolated from pH pool VII of the HF-peptide library. Using the RIA HCC-1 immunoreactive material was purified in 4 successive chromatographic steps. Analysis of the last C_4 RP-HPLC step by ESMS and CZE identified predominantly fractions containing nonglycosylated HCC-1 (1–74) in high purity. These fractions were pooled and lyophilized. The peptide amount was 34 mg based on the purification from 5000 L

Table 1: Mass Spectrometric Analysis of Glycosylated HCC-1^a

sample	HPAE-PAD	theor. Mw	MALDI	ESMS	ΔHF-9621
glycosylated HCC-1		9620.6	9621.2	9621.7	
+neuraminidase	NANA	9038.0	9039.6		582.2 (2 × NANA)
+neuraminidase + O-glycosidase	NANA, GalNAcGal	8673.7	8675.6		946.3 (2 × NANA, GalNAcGal)

^a Mass spectrometric results of neuraminidase and glycosidase treated glycosylated HCC-1 (neuraminic acid = NANA; galactose = Gal; N-acetylgalactosamine = GalNAc). Theoretical average masses are given.

Table 2: Molecular Forms of HCC-1^a

peptide	N-terminal sequence	theor. Mw	detected Mw	glycosylation
HCC-1 (1–74)*	TKTESSSRGP	8673.7	8672.1	
HCC-1 (1–74)	TKTESSSRGP	9620.6	9621.7	O-glycosylated at Ser-7
HCC-1 (3–74)	TESSSRGPYH	8444.5	8442.9	
HCC-1 (4–74)	ESSSRGPYHP	8343.4	8341.9	

^a Identified molecular forms of HCC-1. The N-terminal sequence, theoretical average and detected Mw are given. Nonglycosylated HCC-1 was also detected in the supernatant of HUH-7 hepatoma cell line (*).

of HF. The amino acid sequence analysis confirmed these peptides as HCC-1 (1–74).

HPLC-fractions which contained several different molecular masses and did not show a single peak in the CZE were pooled and rechromatographed on an analytical cation exchange chromatography column and further purified using an analytical C₄ RP-HPLC column. Amino acid sequencing of the immunoreactive material revealed 3 different sequences, namely TKTESSSRGP, TESSSRGPYH, and ESSSRGPYHP. These sequences were identified as truncated N-termini of HCC-1. ESMS of the purified material revealed three molecular masses 8672.1 ± 1.7 Da, 8442.9 ± 1.7 Da, and 8341.9 ± 1.7 Da consistent with the theoretical average Mw of 8673.7 Da for HCC-1 (1–74), 8444.5 Da for HCC-1 (3–74), and 8343.4 Da for HCC-1 (4–74), respectively. These results depict the existence of N-terminally truncated HCC-1 (3–74) and HCC-1 (4–74) circulating in blood plasma.

DISCUSSION

The present study demonstrates that native HCC-1 displays heterogeneity in the circulation with respect to glycosylation as well as to the N-terminal amino acid sequence. By the use of a highly specific HCC-1 RIA and Western blot analysis nonglycosylated HCC-1 (1–74), glycosylated HCC-1 (1–74) as well as N-terminally truncated HCC-1 (3–74), HCC-1 (4–74) were identified in human hemofiltrate.

Identification of different molecular forms of HCC-1 (Table 2) is not derivable from the chromatography of human plasma with a single peak of IR–HCC-1 (Figure 1A) as well as from the mass spectrometric analysis of IR–HCC-1 purified from human plasma which suggested a single molecular form of HCC-1 (Figure 1D). This effect may be due to the following reasons: 1) HCC-1 (1–74), HCC-1 (3–74), HCC-1 (4–74) and glycosylated HCC-1 display the same retention behavior on the semipreparative RP column. 2) Compared to total HCC-1 there is only a low percentage of HCC-1 (3–74) and HCC-1 (4–74) in hemofiltrate not detectable by mass spectrometric analysis or Western blot analysis. Estimation of the purification procedure suggests

that approximately 3% of total HCC-1 is HCC-1 (3–74) and approximately 1% is HCC-1 (4–74), respectively.

Glycosylated HCC-1 was identified by the use of amino acid sequencing identifying the N-terminus. The molecular mass of the isolated peptide measured by ESMS was found to be 9,621.7 Da, a difference of 946 Da to that of HCC-1. An N-terminal extension of the peptide by additional amino acids is not likely since HCC-1 is coded for by a mRNA with a stop codon following the last amino acid of the circulating peptide (Asp-74). Glycosylation of HCC-1 (1–74) was identified at Ser-7. The additional 946 Da in glycosylated HCC-1 consist of an O-glycosidic modification of Ser-7. Whereas O-glycosidase specifically decomposes Gal-β(1–3)GalNAc units from glycopeptides neuraminidase hydrolyzes terminal N- or O-acyl-neuraminic acids that show α2–3, α2–6 or α2–8 bonds. R – GalNAc[–(α2–6)-NANA]–(β1–3)-Gal(α2–3)-NANA is a common core structure which is often found in O-glycosylated proteins and peptides, e.g. in IL-2 (9). Our findings suggest that HCC-1 exhibit such a glycosylation site (Figure 3). The glycosylation site Ser-7 of HCC-1 is surrounded by two serines in position 5 and 6, threonines in position 1 and 3 and proline in position 10. This is in correspondence to Elhammer et al. (10) who showed that O-glycosylation sites were found to be surrounded by proline, serine, and threonine residues with increased frequency in positions –4 to +4 of the glycosylation site. Additionally proline in position 10 corresponds to the finding of Wilson et al. (11) who showed increased frequency of proline residues at positions –1 and +3 relative to the O-glycosylation sites.

Whereas glycosylated HCC-1 was not detectable by MALDI-MS analysis of the plasma samples Western blot analysis displayed a band which is migrating with purified native glycosylated HCC-1 (Figure 1E). This suggests that glycosylated HCC-1 is not exclusively found in patients with chronic renal failure but circulates in blood plasma of healthy subjects.

Western blot analysis of IR–HCC-1 produced by the human hepatoma cell line HUH-7 detected only nonglycosylated HCC-1 fortifying that this molecule is endogenously produced but not generated as an artifact during the purification procedures. Production of HCC-1 by HUH-7 cells is in accordance with the high expression of HCC-1-message found in these cells and in the liver (1). As expected for a constitutively expressed peptide, no storage of HCC-1 in HUH-7 cells could be detected by Western blotting using peptide extracts from these cells (data not shown).

Concerning the physiological relevance of the glycosylation preliminary results indicate that both HCC-1 (1–74) and glycosylated HCC-1 (1–74) induce changes of cytosolic free Ca²⁺ in human monocytes with the same potency. This is in accordance with investigations of Kameyoshi et al. (12) who identified N-terminal O-glycosylation of RANTES, an

other CCR-1 agonist. The derivatization of RANTES at serine residue 4 or 5 did not affect chemotactic activity on eosinophiles.

That the N-terminus of HCC-1 is important for its biological activity was currently found by Tsou et al. (3) who demonstrated that truncated HCC-1 (4–74) and HCC-1 (6–74) is more potent in inhibition of adenylyl cyclase in CCR-1 transfected HEK-293 cells and exhibits stronger chemotactic activity than HCC-1 (1–74). Since nonspecific degradation of HF peptides during collection of hemofiltrate and preparation of the peptide library is widely excluded (13), the identification of truncated HCC-1 (3–74) and HCC-1 (4–74) in hemofiltrate suggests that the processing of the HCC-1 N-terminus occurs in vivo enhancing the biological activity of HCC-1.

Modulation of the biological activity by the N-terminal structure is also suggested by comparison of HCC-1 with MIP-1 α , which exhibits the highest homology to HCC-1 with 46%. Whereas between the first and the last cysteine residue the homology is 61%, the N-terminal region shows a homology of 13% whereby HCC-1 exhibits 15 N-terminal amino acids and MIP-1 α 10 amino acids. This may explain the reduced affinity of HCC-1 to the CCR-1 receptor with an IC₅₀ of about 90 nM versus 1.3 nM for MIP-1 α (3) and in part the higher potency of MIP-1 α to induce calcium flux and induction in monocytes. The importance of N-terminal modifications in chemokines was also demonstrated for other chemokines that can change receptor and target cell selectivity, increase or decrease biological activity, or change an agonist to an antagonist. For example the three major forms of CK β -8 showed a large variation in their potency to mobilize intracellular calcium (14). N-terminally truncated RANTES (3–68) inhibited infection of PBMC by M-tropic HIV-1 strains 10-fold more efficiently than intact RANTES (15). Antagonistic activity was shown for posttranslationally modified MCP-2 (6–76) which could completely block the chemotactic effect of intact MCP-2 (16). Endothelium derived N-terminally truncated CXC chemokine IL-8 was found to be an apoptotic factor for leukemic cells, whereas intact IL-8 bears no apoptotic activity (17, 18).

In conclusion, our findings suggest that HCC-1 circulates as nonglycosylated, glycosylated as well as N-terminally truncated peptides in the blood. Identification of these peptides suggests that a specific processing of the N-terminus may exist in vivo which influences the biological activity of HCC-1.

ACKNOWLEDGMENT

We wish to thank Dr. Marie-Luise Hagmann, Boehringer Mannheim GmbH, Penzberg, Germany, for carbohydrate

analysis and Ulrike Schrameck, Ilka Uhrlandt, Susanne Hollrieder, and Jutta Barras-Akhnoukh for expert technical assistance.

REFERENCES

- Schulz-Knappe, P., Mägert, H.-J., Dewald, B., Meyer, M., Cetin, Y., Kubbies, M., Tomeczkowski, J., Kirchhoff, K., Raida, M., Adermann, K., Kist, A., Reinecke, M., Sillard, R., Pardigol, A., Uguccioni, M., Baggiolini, M., and Forssmann, W. G. (1996) *J. Exp. Med.* 183, 295–299.
- Zlotnik, A., Morales, J., and Hedrick, J. (1999) *Crit. Rev. Immunol.* 19, 1–47.
- Tsou, C., Gladue, R., Carroll, L., Paradis, T., Boyd, J., Nelson, R., Neote, K., and Charo, I. (1998) *J. Exp. Med.* 188, 603–608.
- Polson, A., Coetzer, T., Kruger, J., von Maltzahn, E., and van der Merwe, K. (1985) *Immunol. Invest.* 14, 323–327.
- Schägger, H., and von Jagow, G. (1987) *Anal. Biochem.* 166, 368–379.
- Forssmann, W. G., Schulz-Knappe, P., Meyer, M., Adermann, K., Forssmann, K., Hock, D., and Aoki, A. (1993) in *Proceedings of the 2nd Japan Symposium on Peptide Chemistry* (Yanaihara, N., Ed.) pp 553–557, Escom, Leiden.
- Schulz-Knappe, P., Schrader, M., Ständker, L., Richter, R., Hess, R., Jürgens, M., and Forssmann, W. G. (1997) *J. Chromatogr. A* 776, 125–132.
- Karas, M., and Hillenkamp, F. (1988) *Anal. Chem.* 80, 2299–2301.
- Conradt, H., Nimtz, M., Dittmar, K., Lindenmaier, W., Hoppe, J., and Hauser, H. (1989) *J. Biol. Chem.* 264, 17368–17373.
- Elhammer, A., Poorman, R., Brown, E., Maggiora, L., Hoogerheide, J., and Keady, F. (1993) *J. Biol. Chem.* 268, 10029–10038.
- Wilson, I., Gavel, Y., and von Heijne, G. (1991) *Biochem. J.* 275, 529–534.
- Kameyoshi, Y., Dörschner, A., Mallet, A., Christophers, E., and Schröder, J. (1992) *J. Exp. Med.* 176, 587–592.
- Richter, R., Schulz-Knappe, P., Schrader, M., Standker, L., Jürgens, M., Tamm, H., and Forssmann, W. G. (1999) *J. Chromatogr. B, Biomed. Sci. App.* 726, 25–35.
- Macphree, C., Appelbaum, E., Johanson, K., Moores, K., Imburgia, C., Fornwald, J., Berkhout, T., Brawner, M., Groot, P., O'Donnell, K., O'Shannessy, D., Scott, G., and White, J. (1998) *J. Immunol.* 161, 6273–6279.
- Schols, D., Proost, P., Struyf, S., Wuyts, A., De Meester, I., Scharpe, S., Van Damme, J., and De Clercq, E. (1998) *Antiviral Res.* 39, 175–187.
- Proost, P., Struyf, S., Couvreur, M., Lenaerts, J., Conings, R., Menten, P., Verhaert, P., Wuyts, A., and Van Damme, J. (1998) *J. Immunol.* 160, 4034–4041.
- Terui, Y., Ikeda, M., Tomizuka, H., Kasahara, T., Ohtsuki, T., Uwai, M., Mori, M., Itoh, T., Tanaka, M., Yamada, M., Shimamura, S., Miura, Y., and Hatake, K. (1998) *Biochem. Biophys. Res. Commun.* 243, 407–411.
- Terui, Y., Ikeda, M., Tomizuka, H., Kasahara, T., Ohtsuki, T., Uwai, M., Mori, M., Itoh, T., Tanaka, M., Yamada, M., Shimamura, S., Ishizaka, Y., Ikeda, K., Ozawa, K., Miura, Y., and Hatake, K. (1998) *Blood* 92, 2672–2680.

BI992488Q